Contents lists available at ScienceDirect

Ecotoxicology and Environmental Safety

High methylmercury uptake by green algae in Lake Titicaca: Potential implications for remediation

Roxana Quiroga-Flores [a,b,*], Stéphane Guédron [c], Dario Achá [d]

[a] Instituto de Investigaciones Fármaco Bioquímicas, Universidad Mayor de San Andrés, La Paz, Bolivia
[b] Division of Biotechnology, Department of Chemistry, P.O. Box 124, Lund University, SE-223 62, Lund, Sweden
[c] Univ. Grenoble Alpes, Univ. Savoie Mont Blanc, CNRS, IRD, IFSTTAR, ISTerre, 38000, Grenoble, France
[d] Laboratorio de Calidad Ambiental, Instituto de Ecología, Universidad Mayor de San Andrés, Campus Universitario de Cota Cota, Casilla, 3161, La Paz, Bolivia

ABSTRACT

Anthropogenic pressure in the high altitude lakes such as Titicaca and Uru (Bolivia) may favor the production of methylmercury (MeHg) known to accumulate in trophic chains. Periphyton associated with emerged aquatic plants (totoras) from the lake shores accumulates and demethylates MeHg providing a potential cost-effective water treatment technique. In this laboratory study, we measured the MeHg uptake kinetics of a consortium of green algae isolated from Lake Titicaca totora's periphyton. The most abundant algal consortium, composed of *Oedogonium* spp., *Chlorella* spp., *Scenedesmus* spp., was exposed to rising MeHg concentrations (from 5 to 200 $ng \cdot L^{-1}$) to assess their maximum potential capacity for MeHg accumulation. Various algal biomass concentrations were tested to choose the optimal one. Results provided a net MeHg uptake rate by this algal consortium of 2.38 amol $ng^{-1} \cdot h^{-1} \cdot nM^{-1}$ (the total uptake was 2863 ng MeHg·g^{-1}) for an initial concentration of 200 ng MeHg·L^{-1} with an algal biomass concentration of 0.02 g·L^{-1}. This initial MeHg concentration is 1000 times higher than the one measured in the eutrophic Cohana Bay of Lake Titicaca, which shows the high accumulation potential of these green algae. Our data suggest that periphyton has a high potential for the treatment of Hg contaminated waters in constructing wetlands in the Andean Altiplano.

1. Introduction

Methylmercury (MeHg) is one of the most toxic species of mercury (Hg). The neurotoxicity effects of MeHg in both humans and animals vary from severe cerebral palsy to mental developmental delays (Castoldi et al., 2001). In aquatic environments, microorganisms such as sulfate-reducing bacteria (Achá et al., 2011), iron-reducing bacteria (Fleming et al., 2006), and methanogens (Correia et al., 2012) mediate most Hg methylation in suboxic and anoxic environments. High variation in Hg methylation rates has been reported in lake compartments such as sediments, water column, benthic biofilms and periphyton (Achá et al., 2012; Bouchet et al., 2011; Correia et al., 2012; Dranguet et al., 2017; Lanza et al., 2017).

Periphyton is a complex matrix composed of an assemblage of organisms (e.g., algae, fungi, prokaryotes, and protozoa) embedded in an exopolysaccharide matrix attached to macrophytes (Correia et al., 2012; Lázaro et al., 2013). In the Bolivian high altitude lakes, such as lakes Titicaca and Uru-Uru, periphyton associated with emerged aquatic plants (*Schoenoplectus totoras* also called "totoras") was reported to be a weak producer of MeHg (Bouchet et al., 2018). Furthermore, the algae *Oedogonium* spp. was the most influential group for MeHg accumulation in Lake Uru-Uru totora's periphyton (Lanza et al., 2017). Such findings are in accordance with *in vitro* studies with pure algae cultures, which suggested that the physiological configuration of chloroplasts in green algae could enhance Hg accumulation (Miles et al., 2001; Moye et al., 2002). In addition, *in situ* incubations performed with isotopically enriched Hg species in both lakes Titicaca and Uru-Uru, have shown evidence that demethylation was dominant in totora's periphyton (Bouchet et al., 2018).

In the Bolivian Andean Altiplano, the levels of MeHg in aquatic ecosystems are rising resulting from anthropogenic induced Hg contamination and eutrophication (Achá et al., 2018; Alanoca et al., 2016b; Bouchet et al., 2018; Guédron et al., 2017; Lanza et al., 2017). In particular, intense methylation was found in epibenthic biofilms, while it remained low in sediments and aquatic plant's periphyton (Alanoca et al., 2016a; Bouchet et al., 2018; Lanza et al., 2017).

---

* Corresponding author. Instituto de Investigaciones Fármaco Bioquímicas, Universidad Mayor de San Andrés, La Paz, Bolivia.
E-mail address: roxana.quirogaf@gmail.com (R. Quiroga-Flores).

The capacity of periphyton to bioaccumulate MeHg may have ecological implications for biomagnification because it is one of the main primary food source for aquatic organisms (invertebrates and fish) in the Andes and Amazonia (Lázaro et al., 2013; Molina et al., 2010). However, the same bioaccumulation capacity of periphyton could also be used for remediation purposes. Periphyton may become an interesting low-cost water treatment alternative if the accumulating organisms are removed at the end of the process.

In this laboratory study, we conducted MeHg uptake kinetics with a consortium of green algae isolated from Totora's periphyton collected in Lake Titicaca at various algal biomass and MeHg concentrations. We provide new insights into the proportion of MeHg accumulated inside and on the cell membrane and identified the potential binding sites on the membrane by Fourier-transform infrared spectroscopy (FTIR). Finally, we discuss the potential application of periphyton's green algae as a remediation technique for the Bolivian Andes.

2. Materials and methods

2.1. Algae cultivation and identification

Periphyton was collected from the shoots of totora sedges (i.e., *Scheanoplectus californicus*) in the Cohana Bay (Lake Titicaca, Bolivia, 3809 m above sea level, $16°20'40.13''S$; $68°44'8.12''W$) into 50-mL sterile PET tubes and stored and transported in a portable cooler at $4 °C$ to the laboratory (within 3 h) for further analysis and cultivation. In the laboratory, periphyton samples were inoculated and cultivated in the autoclaved Alga-Gro® (Carolina Biological Supply Company) freshwater medium (pH $7.20 \pm 1 °C$) under constant fluorescent light. After sub-culturing five times, with an interval of 5–6 days, aliquots were taken and fixed with formaldehyde (1% v/v) to identify algae genera using a microscope (Microscope AmScope, microscope digital camera 5.1 MP, China). Amongst the consortia cultivated in the Alga-Gro® medium, the consortium with the most abundant *Oedogonium* spp. was selected for the uptake experiments. Triplicates of freeze-dried algae samples (Finni-aqua, Lyovac GT2, Leybold, Trivac, Germany) were used to determine the dry weight of algae and calculate the algal biomass concentrations (expressed as $g \cdot L^{-1}$).

The relative abundance of the algae (%) in the consortium was determined based on their cell volume (i.e. biovolume). The dimensions of the algal cells were obtained by the ImageJ 1.52a software (USA), which were converted to their respective biovolume, followed by cell counting, as described by Wetzel and Likens (2000). Direct count under the microscope was applied to unicellular organisms, and the abundance of colonies and filamentous algae was expressed as cells per colony or filament. The biovolume was determined using total cells present in either colonies or filaments. The total organic carbon of the biomass (mM C) present in the uptake experiment was estimated from the total biovolume of algae (μm^3).

2.2. Methylmercury uptake experiments

To test the optimal algal biomass concentration (i.e., the algal dosage providing the highest percentage of MeHg removal from the solution), methylmercury uptake experiments were first conducted using three dosages of algae, i.e. 0.005, 0.01, and 0.02 $g \cdot L^{-1}$ in a 40 mL solution of Alga-Gro® freshwater medium spiked with methylmercury chloride (CH$_3$HgCl) to obtain a final concentration of 10 ng MeHg$\cdot L^{-1}$. The experiment was run at a temperature of $16.5 \pm 0.5 °C$, and the average pH of the solution was 6.8 ± 0.3. Samples were collected at 0, 0.17, 0.3, 0.5, 0.75, 1, 1.5, 2, 3, 6 and 24 hours (h), and filtered with polytetrafluoroethylene (PTFE) filter membranes (0.22 μm pore size) and acidified with HCl (1% v/v, Sigma-Aldrich Suprapure grade) prior to MeHg analysis. Abiotic controls were run in duplicates without algal biomass and sampled at 0, 6, and 24 h, to calculate the abiotic loss of MeHg. The MeHg uptake (U$_t$, expressed in ng MeHg$\cdot g^{-1}$ algae) was calculated for each given time and was considered as the amount of MeHg transferred from the aqueous phase to the algal biomass. The total uptake of MeHg (U$_{Total}$, expressed in ng MeHg$\cdot g^{-1}$ algae) was calculated at the end of the kinetic experiment. The U$_t$ data were then plotted versus time to calculate the MeHg uptake rate (U$_R$, in ng MeHg$\cdot g^{-1}$ algae$\cdot h^{-1}$).

The chosen optimal algal biomass concentration was then used to test the maximum MeHg uptake capacity at initial MeHg concentrations in the solution of 5, 10, 20, 40, 80, 100, and 200 ng$\cdot L^{-1}$. Samples were collected at 0 and 6 h for the calculation of the U$_{Total}$ and the net uptake rate (i.e., U$_{Total}$ normalized to the MeHg concentration tested, expressed in amol$\cdot ng^{-1} \cdot h^{-1} \cdot nM^{-1}$).

The fraction of MeHg bound extracellularly was determined at t = 6 h of the MeHg uptake experiments performed with 10 ng MeHg$\cdot L^{-1}$ following the protocol reported by Beauvais-Flück et al. (2017) using 4 mM EDTANa$_2$ (Sigma-Aldrich). EDTA was added to the culture tube and was agitated for 30 min. Thereafter, samples (MeHg$_{EDTA,t=6}$) were collected and filtered before MeHg analysis. Control algal cultures without the addition of EDTA were run in parallel and sampled at 0 and 6 h, which were denominated as MeHg$_{control,t=0}$, and MeHg$_{control,t=6}$, respectively. The intracellular MeHg (MeHg$_I$) was calculated as follows: MeHg$_I$ = MeHg$_{control,t=0}$ - MeHg$_{EDTA,t=6}$, whereas the extracellular MeHg (MeHg$_E$) was calculated as: MeHg$_E$ = MeHg$_{control,t=0}$ - MeHg$_{control,t=6}$ - MeHg$_I$. The result is presented as the MeHg$_E$:MeHg$_{total}$ ratio.

2.3. Analytical methods

2.3.1. Methylmercury analysis

All materials in contact with the samples were previously acid-washed following the ultra-clean protocols (Cossa et al., 2003). Methylmercury was determined after derivatization by purge and trap-gas chromatograph-cold vapor atomic fluorescence spectrometry (MERX System, Brooks Rand®). Briefly, blanks, standards, and samples were added to 40 mL-amber vials containing ultrapure water buffered at pH 4.5 and the ethylating agent NaBEt$_4$ (Guédron et al., 2014). MeHg contents for all samples were run in duplicates and controlled using the standard addition technique (Guédron et al., 2014). Because no liquid MeHg CRM is available, MeHg measurements traceability and accuracy were checked against ERM CC580 CRM (IRMM - Institute for Reference Materials and Measurements). MeHg concentrations measured for this CRM (75.9 ± 4.9 ng Hg$\cdot g^{-1}$, N = 9) were within 10% of the certified values (75 ± 4 ng Hg$\cdot g^{-1}$). The measurement error on replicates was usually about 10% and was always lower than 15%. The blanks (MQ water and AlgaGro® medium) were always below 20 pg$\cdot L^{-1}$ (N = 39), the quantification limit (3SDblk) was 0.004 ng$\cdot L^{-1}$, and the absolute detection was 0.001 ng$\cdot L^{-1}$ of MeHg.

2.3.2. Fourier transformed infrared spectroscopy

Potential binding sites in the surface of the membrane of algae were determined on freeze-dried samples by a Fourier-transform infrared Nicolet iS5 ATR spectrometer (FTIR, Thermo Scientific, Sweden). The presented data is a single-averaged spectrum of 16 scans with a frequency of 4 cm^{-1} analyzed in the range of 4000–400 cm^{-1}. The data was processed in the Omnic software version 8.3 (Thermo Scientific, Sweden).

2.4. Statistical tests

The normal distribution of the data was evaluated with the Shapiro-Wilk test. When data followed a normal distribution, a one-way analysis of variance (ANOVA) test was performed (i.e., for data of kinetics and abiotic loss). Tukey HSD test was performed to detect significant differences between the data sets. The Pearson correlation test was used for the correlation in the maximum MeHg uptake experiments. P values below 0.05 were considered significant. All statistical analyses were processed with R software, version 3.4.1 (Team, 2013).

3. Results and discussion

3.1. Methylmercury uptake kinetics

The periphyton's green algae consortium had abundant filamentous *Oedogonium* spp., coccoid *Chlorella* spp., and the 4-cells colony *Scenedesmus* spp. (Fig. S1). In terms of biovolume (μm^3), the abundance of *Oedogonium* spp. was 54%, followed by *Chlorella* spp. (40%) and *Scenedesmus* spp. (6%). Table S1 shows more details about cell count and biovolume. The total organic carbon present in the biomass of algae was estimated using the relationship between carbon and cell volume reported by Wetzel and Likens (2000), where 1 pg C = 0.16·biovolume (μm^3) in the case of Chlorophytes (Wetzel and Likens, 2000). Thus, the organic carbon concentration present in algal biomass of 0.02 g·L^{-1} was 0.1 mM C. The slight presence of bacteria observed microscopically may have grown at the expense of the algal biomass decay. The dissolved organic matter (DOM) may have changed slightly during the experiment, but it should be safe to assume that DOM originates mainly from the algae consortium. AlgaGro® does not contain dissolved organic carbon, according to the manufacturer.

During the kinetic experiments, the abiotic loss of MeHg was found significant (33%) after 24 h ($p < 0.05$), which likely resulted from MeHg adsorption on vial walls or demethylation. For this reason, we only considered the first 6-h interval, where MeHg loss was negligible. The MeHg uptake kinetics experiments (Fig. 1) indicated a rapid increase in MeHg uptake before it tended towards a plateau until the end of the experiment period allowing the calculation of two MeHg uptake rates [Fig. 1; one from 0.08 to 1.5 h (U_{R1}) and the second from 3 to 6 h (U_{R2})].

The calculated uptake rate obtained from the slope of the MeHg uptake during the first 1.5 h (U_{R1} - Fig. 1) was two order of magnitude lower than the rates reported for the algae *Selenastrum capricornutum*, *Thalassiosira* spp., *Schizothrix calcicola*, *Cosmarium botrytis* (Moye et al., 2002, 2003) and for the algae *Chlamydomona reinhardtii* (Pickhardt and Fisher, 2007). However, the uptake rates in their studies were only calculated between initial and final sampling times, with shorter [0.08 h (Moye et al., 2002)] or longer [48 h (Pickhardt and Fisher, 2007)] time of exposures which makes the data difficult to compare. High variability of data for metal bio-uptake kinetics has been reported in the literature for the same algal strain because bio-uptake is a complex process that results from the balance between influx and effluxes rates (Luoma and Rainbow, 2005; Skrobonja et al., 2019). Hence, standardized uptake methods are needed for obtaining comparable data. Based on our results, the calculation of initial-final rates for shorter and longer exposure times can overestimate and underestimate real MeHg uptake rates.

Kinetics using lower algal biomass concentrations (i.e., 0.005 and 0.01 g·L^{-1}) showed similar bi-modal kinetic patterns with small differences in rates (only U_{R1} was compared) and in the total MeHg uptake at the platea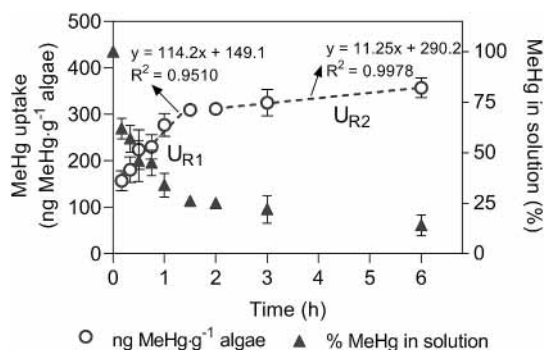u (Fig. 2a). Among the three parameters compared between the three algal biomass concentrations (Fig. 2b), only the percentage of MeHg removed from the solution rose linearly ($R^2 = 0.99$, $p < 0.05$) with increasing algal biomass concentration reaching the highest removal (85%) at the highest algal biomass concentrations (0.02 g·L^{-1}). In opposition, total MeHg uptake (U_{Total}) and the uptake rate (U_{R1}) remained both in a narrow range (e.g. from 340 to 400 ng MeHg·g^{-1} algae - Fig. 2b) with increasing algal biomass concentration. Such stability in the MeHg uptake demonstrates that for the same initial MeHg concentration (10 ng·L^{-1}), the uptake rate is independent of the algal biomass concentration. The optimal algal biomass concentration was 0.02 g·L^{-1} and was selected for the following maximum MeHg uptake experiment performed at various MeHg concentrations.

3.2. Maximum methylmercury uptake potential

To evaluate the maximum MeHg uptake capacity of the algae, we increased the initial concentration of MeHg for a constant algal biomass concentration (0.02 g algae·L^{-1}) and measured the U_{Total} after 6 h of exposure (Fig. 3). The abiotic loss of MeHg for the different concentrations tested after 6 h ranged between 0 and 17%. For the uptake by algae, a linear correlation ($R^2 = 0.99$, $p < 0.05$) was found between the MeHg uptake and increasing initial MeHg concentration until approximately 100 ng·L^{-1}. For the two highest initial MeHg concentrations (100 and 180 ng·L^{-1} – Fig. 3), the MeHg uptake reached a plateau at 2863 ± 142 ng MeHg·g^{-1} algae likely due to the saturation of the adsorption sites on the algal cell membranes.

One cannot exclude a toxic effect on the algae if we consider the internalization of MeHg. The toxicity tolerance varies significantly among algae genera. For example, a reduced growth rate was reported above 17 ng MeHg·L^{-1} for *T. weissglogii* (Mason et al., 1996). Another

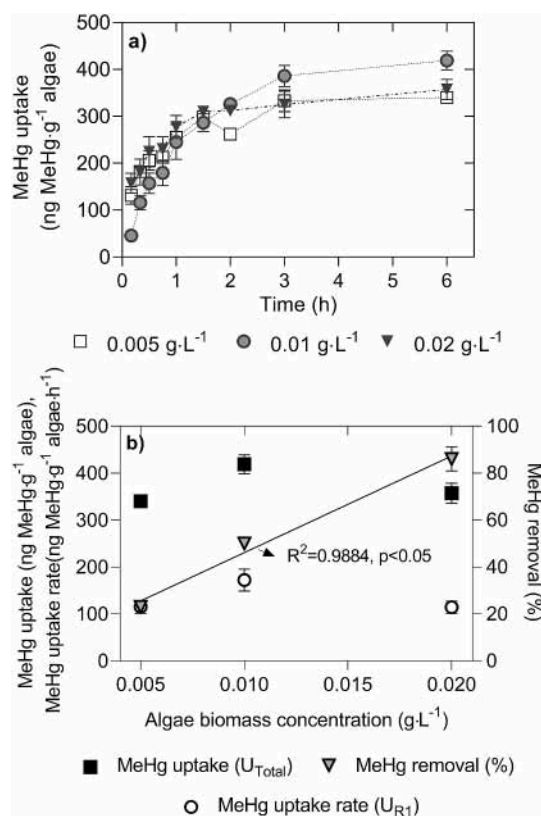**Fig. 2.** A) Kinetics of MeHg uptake at 0.005, 0.01 and 0.02 g algae·L^{-1}. B) Total MeHg uptake (U_{Total}), MeHg uptake rate (U_{R1}) and linear regression of the percentage of MeHg removed from the solution at 0.005, 0.01 and 0.02 g algae·L^{-1}. Initial conditions: MeHg = 10 ng·L^{-1}; pH = 6.8 ± 0.3 and T = 16.5 ± 0.5 °C.

Fig. 1. Kinetics of MeHg uptake (in ng MeHg·g^{-1} algae) at 0.02 g algae·L^{-1} and percentage of MeHg remaining in the solution. The MeHg uptake rates (in ng MeHg·g^{-1} algae·h^{-1}) were calculated from the slope of the regressions. Initial conditions: MeHg = 10 ng·L^{-1}; pH = 6.8 ± 0.3 and T = 16.5 ± 0.5 °C.

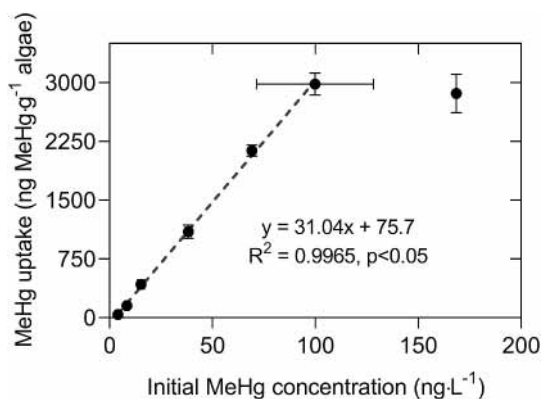**Fig. 3.** Relation between MeHg uptake by algal biomass (ng MeHg·g^{-1} algae) after 6 h of exposure and initial MeHg concentrations; experimental data includes horizontal and vertical error bars. Linear regression was carried out for MeHg concentrations ranging from 5 to 100 ng MeHg·L^{-1}. Initial conditions: MeHg = 5–200 ng·L^{-1}, pCl = 4.5 to 6 (for 200 to 5 ng MeHg·L^{-1}, respectively), pH = 6.8 $\pm$ 0.3, T = 16.5 $\pm$ 0.5 °C, algal biomass concentration: 0.02 g·L^{-1}.

study reported that even at 2.1 ng MeHg·L^{-1} for *C. reinhardtii,* there was dysregulation of genes involved in processes such as energy metabolism, photosynthesis, and redox homeostasis production, although no physiological effects were identified (Beauvais-Flück et al., 2017). In contrast, *Oedogonium* spp. seems to be more tolerant than other algal species as it was found to dominate an algal community after prolonged exposure to 14·10^3 ng Hg$_{total}$·L^{-1} (Dranguet et al., 2017; Val et al., 2016).

The estimated maximum MeHg uptake potential may be over or underestimated compared to environmental conditions. The experiment does not take into account natural DOM, free thiol groups, periphyton matrix, invertebrates and bacteria that may compete for MeHg absorption (Leclerc et al., 2015; Pickhardt and Fisher, 2007; Wang et al., 2018) or changes in MeHg availability for algae and the periphyton itself (Bravo et al., 2018; Skrobonja et al., 2019). Consequently, it must be emphasized that such an estimate is just a potential, and caution is needed for environmental extrapolations. Although DOC was not monitored during the experiment, the dead algal cells may have released DOC to the solution (Bravo et al., 2017) possibly reaching similar levels to those measured in Lake Titicaca (average DOC $\pm$ SD = 3.78 $\pm$ 1.42 mg·L^{-1}) or in the shallow Cohana Bay where concentrations rise up to 8 mg ·L^{-1} (Achá et al., 2018; Guédron et al., 2017, 2020). For comparison purposes, we normalized our rates to the highest initial concentrations of MeHg tested (expressed as amol MeHg·ng^{-1} algae·h^{-1}·nM^{-1}). Table 1 summarizes our data along with other rates reported in the literature. The high variability between these data could be attributed to the inherent uptake capacity of the different species of alga (e.g. type of exudates produced) and to the conditions of MeHg exposure (e.g. initial concentration, duration, pH, pCl and static vs stirring conditions). In our study, the net uptake rates range within the lowest reported values likely resulting from the static culture conditions and the relatively high amount of algae compared to the MeHg added. In contrast, most of the other studies were performed under stirred culture conditions with lower algal concentrations and higher MeHg spikes.

3.3. Assessment of intracellular vs. extracellular methylmercury distribution

The EDTA quantification of MeHg bound to the cell membrane and internalized in the cell after 6 h gave a MeHg$_E$:MeHg$_{total}$ ratio of 0.7, which indicates that at least 70% of MeHg is adsorbed onto the cell walls. This result is consistent with a recent laboratory experiment that reported an average of 78% of MeHg adsorbed on the cell membrane of the green unicellular microalga *Selenastrum capricornutum* (Skrobonja et al., 2019). Lower percentages (between 44 and 52%) were reported

Table 1

Net uptake rates of MeHg reported by other studies using living biomass of algae. Data are presented along with biomass/cells concentration, experimental conditions and references.

Algae	Algal cell/ biomass concentration	Experimental conditions*	Normalized net uptake rate (amol·ng^{-1}·h^{-1}·nM^{-1})
Consortium: Green algae, *Oedogonium* spp *Chlorella* spp. *Scenedesmus* spp.	0.02 g·L^{-1} or 6·10^4 cells·mL^{-1}	200 ng·L^{-1}, pH 6.8, pCl 6, 16.5 $\pm$ 0.5 °C, 6 h, static	[a] 2.38 (This study)
Green algae: *Chlamydomona reinhardtii* (Bravo et al., 2014)	10^5 cells·mL^{-1}	21 ng·L^{-1}, pH 7, 20 °C, 89 % MeHgCl, 48 h, static	[b,c] 0.072
Green algae: *Chlamydomona reinhardtii* (Pickhardt and Fisher, 2007)	0.0005–0.002 g·L^{-1}	160 ng·L^{-1}, pH 7.9, 17 °C, 280 µM C, 48 h, static	[a,d] 17
Green algae: *Selenastrum capricornutum* (Moye et al., 2002, 2003)	0.005 g·L^{-1}	410 ng·L^{-1}, pH 7, pCl 2.2, 20–22 °C, 0.08 h, stirred	[b] 278
Green algae: *Selenastrum capricornutum* (Bouchet and Björn, 2014)	10^5 cells·mL^{-1}	45 707[e] ng·L^{-1}, pH 7.9, 20–21 °C, 45 h, static	[a,f] 0.294
Blue-green algae: *Schizothrix calcicola* (Moye et al., 2002, 2003)	0.005 g·L^{-1}	410 ng·L^{-1}, pH 7, pCl 2.2, 20–22 °C, 0.08 h, stirred	[b] 11.2
Diatom: *Thalassiosira* spp.(Moye et al., 2002, 2003)	0.005 g·L^{-1}	410 ng·L^{-1}, pH 7, pCl 2.2, 20–22 °C, 0.08 h, stirred	[b] 16.7
Diatom: *Thalassiosira. weissflogii* (Mason et al., 1996)	0.005–0.01 g·L^{-1} or 1–2·10^4 cells·mL^{-1}	32 ng·L^{-1}, pH 4.3, pCl 3.3, 20 °C, 4 h, static	[a,g] 36

*Initial MeHg concentration, pH, pCl, temperature, duration and stirring condition.

[a] MeHg accumulated intracellularly and extracellularly.

[b] MeHg accumulated intracellularly.

[c] For conversion from cell to ng, the dry weight per cell was considered equal to 83 pg as reported by Pickhardt (Pickhardt and Fisher, 2007).

[d] Converted from 602.8 nmol·g^{-1}.

[e] Determined by GC-ICPMS, total MeHg was in the form of 4 thiol complexes: 50 nM each of MMHg-2MPA (2-mercaptopropionic acid), MMHg-SULF (mercaptoethanesulfonate), MMHg-Glyc (monothioglycerol), and 83 nM MMHg-Cys (cysteine).

[f] Only the concentration of MMHg-Cys was used for the calculation.

[g] Read from Fig. 4, for conversion of units we used the average of the mass (0.0075 g·L^{-1}).

for the algae *C. reinhardtii* for different initial concentrations of MeHg after 2 h of incubation (Beauvais-Flück et al., 2017). In contrast, negligible MeHg was bound extracellularly after 0.08 h of exposure for the alga *S. capricornutum* and *C. botrytis* (Miles et al., 2001). The predominance of MeHgOH species and low thiols concentrations have been associated with higher MeHg fractions bound extracellularly (Skrobonja et al., 2019). Such might be the case in our study as the medium had no other source of TOC besides the algae itself and low concentration of Cl$^-$ (pCl = 6). Moye et al. (2003) proposed that the internalization of MeHg

was mainly associated with active transport involving transporters in the membrane. As carriers are saturable, we cannot rule out that MeHg internalization may fluctuate during a kinetic experiment.

The biomass was analyzed by FTIR (Fig. S2) to get an insight into potential binding sites available extracellularly. Seven stretch bands were identified indicating the presence of amines, carboxyl and lipids and/or saturated aliphatic chains, saccharides, thioethers and disulfides, and thiosulfates (Coates, 2000; D'Souza et al., 2008; Giordano et al., 2001) which are consistent with reported functional groups of the external cellulosic wall for green algae (Sheath and Wehr, 2015). Amongst these groups, thioethers (R-S-R) and disulfides (R–S–S–R′) are functional groups present in compounds such as methionine and glutathione, and R-cysteine-cysteine-R′ respectively (Krauss and Schmidt, 1987). These compounds are the most likely binding sites for MeHg given its high affinity for reduced thiols and sulfonates (Dranguet et al., 2017; Skrobonja et al., 2019; Wang et al., 2018). Based on such a hypothesis, our assessment of the proportion of extracellular MeHg may be underestimated because thiols could have outcompeted EDTA.

3.4. Perspectives on sustainable wastewater treatment techniques in Lake Titicaca

In lakes of the Bolivian Andean Altiplano (i.e., Titicaca and Uru-Uru), recent rising anthropogenic pressure (i.e., mining effluent and wastewaters) resulted in the rise of Hg contamination and eutrophication of these aquatic ecosystems (Alanoca et al., 2016b; Guédron et al., 2017). In particular, recent studies in Lake Titicaca highlighted rising levels of MeHg in surface water resulting from both the leaching of coastal urban and agricultural areas and discharges of untreated wastewaters from the Katari River into Cohana Bay (Achá et al., 2018). In the absence of efficient wastewater treatment, constructed wetland using totoras and its associated periphyton appears to be a relevant alternative to reduce contaminant inputs (Sarret et al., 2019).

The MeHg concentrations used in this study are one to three orders of magnitude higher than reported levels in water for lakes of the Andean Altiplano (i.e. Lake Titicaca and Uru-Uru) or other polluted surface water of lakes and rivers around the world (Tab. S2) which range from 0.003 to 1.03 ng·L^{-1}. The range of MeHg concentrations at the inlet of the Katari River to Lake Titicaca's Cohana Bay was reported to be from 0.01 to 0.18 ng·L^{-1} (Achá et al., 2018). Consequently, we estimated the theoretical water flow (Q) needed to remove all MeHg present in 1 L of water with an algal biomass concentration of 0.02 g·L^{-1} (C$_{algae}$) and a MeHg uptake rate (U$_R$) of 0.032 ng MeHg·g^{-1}·s^{-1} (all details of calculations in S.I.4). The obtained Q for removing all MeHg in 1 L for the stated range of concentration is 0.004 and 0.064 L·s^{-1}. These flows are low compared to those reported for constructed wetlands used in the treatment of heavy metals [0.7–2.15 L·s^{-1} (Mays and Edwards, 2001; Mitsch and Wise, 1998)]. The flows in Cohana bay are even higher as the Katari River flows into the Bay with an average flow ranging between 900 L·s^{-1} during the dry season up to 41 000 L·s^{-1} during the rainy season (Archundia et al., 2016). Hence, the alternatives to improve the efficiency of such constructed wetlands would require a higher concentration of biomass, which means increasing the density of totoras stems to promote a higher density of periphyton on their stems. Such an approach would also increase the turbulence and probably increase the scavenging capacity of periphyton.

It is worth mentioning that, although water flow rates incoming from the Katari River are elevated, the high uptake capacity of green algae (2863 ng MeHg·g^{-1} algae) could be key to lower these MeHg fluxes. For example, for a mean MeHg concentration of 0.1 ng·L^{-1}, the amount of MeHg to be treated per day would be between 8 and 354 mg MeHg for the range of Katari water flow (0.07–3.5·10^9 L·day^{-1}). Biomass of 20 g of algae in 1000 L (C$_{algae}$ = 0.02 g·L^{-1}) can uptake up to 57.3 µg MeHg until reaching saturation and treating up to 5.7·10^5 L. These values can be otherwise written as 57.3 µg MeHg·m^{-3}. Therefore, for treating 8 mg MeHg, a wetland would need an effective volume of 136 m^3, which is in the range of some reported wetlands in the literature [85–182 m^3 (Liu et al., 2016)]. Higher net uptakes, such as 354 mg MeHg, need to be addressed by increasing algal biomass.

Yet, the only hindsight we have about such a bioremediation approach concerns dried biomass of the alga *Oedogonium* spp., which has been used to treat water contaminated with Ni (Gupta et al., 2010), Pb (Gupta and Rastogi, 2008a), Cd (Gupta and Rastogi, 2008b) and Cr (Gupta and Rastogi, 2009), but to our knowledge, no information is available on living algae biomass. Furthermore, we still need a better understanding of factors controlling Hg accumulation in the periphyton, which is a complex community of algae, invertebrate and microorganisms. Some studies with similar periphyton suggest that algae are a good starting point to understand MeHg accumulation in periphyton (Lanza et al., 2017). Further geoengineering studies are required to dimension and test the efficiency of such a treatment system. In addition, totora and its periphyton should be removed and renewed to maintain the efficiency of the system and prevent trophic transfer.

4. Conclusion

Our study confirms the reported high capacity of periphyton's algae to uptake MeHg in aquatic ecosystems of the high altitude Andean Altiplano. The lack of laboratory - standardized methods for evaluating contaminants uptake by algae makes the comparison of published results difficult, and methodological developments are still needed. We propose to include the consideration of time of exposure to allow and encourage researchers to report their data normalized by the concentration tested and reported in amol·ng^{-1}·h^{-1}·nM^{-1}. Loss rates and growth rates (if long periods of exposure are used) should also be considered to model the kinetic data correctly. Green algae, in general, have shown higher uptake capacity than other algal genera. Still, most of the studies discuss this potential only concerning the impact in the environment as an entry point of MeHg in biota. We here propose a different approach, using this high MeHg sorption capacity for remediation purposes and applications in the field of constructed wetlands. Further studies are still needed regarding the fate of mercury and methylmercury after adsorption onto periphyton. The treatment of the withdrawn exhausted biomass also needs to be carefully considered with regard to implementation.

References

Achá, D., et al., 2018. Algal bloom exacerbates hydrogen sulfide and methylmercury contamination in the emblematic high-altitude lake Titicaca. Geosciences 8, 438.
Achá, D., et al., 2012. Sulfate-reducing bacteria and mercury methylation in the water column of the lake 658 of the experimental lake area. Geomicrobiol. J. 29, 667–674.

Achá, D., et al., 2011. Importance of sulfate reducing bacteria in mercury methylation and demethylation in periphyton from Bolivian Amazon region. Chemosphere 82, 911–916.

Alanoca, L., et al., 2016a. Diurnal variability and biogeochemical reactivity of mercury species in an extreme high-altitude lake ecosystem of the Bolivian Altiplano. Environ. Sci. Pollut. Control Ser. 23, 6919–6933.

Alanoca, L., et al., 2016b. Synergistic effects of mining and urban effluents on the level and distribution of methylmercury in a shallow aquatic ecosystem of the Bolivian Altiplano. Environ. Sci. J. Integr. Environ. Res.: Process. Impact. 18, 1550–1560.

Archundia, D., et al., 2016. How uncontrolled urban expansion increases the contamination of the Titicaca Lake basin (el alto, La paz, Bolivia). Water, Air, Soil Pollut. 228, 44.

Beauvais-Flück, R., et al., 2017. Cellular toxicity pathways of inorganic and methyl mercury in the green microalga Chlamydomonas reinhardtii. Sci. Rep. 7, 8034.

Bouchet, S., Björn, E., 2014. Analytical developments for the determination of monomethylmercury complexes with low molecular mass thiols by reverse phase liquid chromatography hyphenated to inductively coupled plasma mass spectrometry. J. Chromatogr. A 1339, 50–58.

Bouchet, S., et al., 2011. An experimental approach to investigate mercury species transformations under redox oscillations in coastal sediments. Mar. Environ. Res. 71, 1–9.

Bouchet, S., et al., 2018. Linking microbial activities and low-molecular-weight thiols to Hg methylation in biofilms and periphyton from high-altitude tropical lakes in the Bolivian Altiplano. Environ. Sci. Technol. 52, 9758–9767.

Bravo, A.G., et al., 2017. Molecular composition of organic matter controls methylmercury formation in boreal lakes. Nat. Commun. 8, 1–9.

Bravo, A.G., et al., 2018. The interplay between total mercury, methylmercury and dissolved organic matter in fluvial systems: a latitudinal study across Europe. Water Res. 144, 172–182.

Bravo, A.G., et al., 2014. Species-specific isotope tracers to study the accumulation and biotransformation of mixtures of inorganic and methyl mercury by the microalga Chlamydomonas reinhardtii. Environ. Pollut. 192, 212–215.

Castoldi, A.F., et al., 2001. Neurotoxicity and molecular effects of methylmercury. Brain Res. Bull. 55, 197–203.

Coates, J., 2000. Interpretation of infrared spectra, a practical approach. Encycl. Anal. Chem. 12, 10815–10837.

Correia, R.R.S., et al., 2012. Mercury methylation and the microbial consortium in periphyton of tropical macrophytes: effect of different inhibitors. Environ. Res. 112, 86–91.

Cossa, D., et al., 2003. Dissolved Mercury Speciation in Marine Waters. Analysis Methods in Marine Environment. Ifremer and French Ecology. Durable Development Ministry (in French).

D`Souza, L., et al., 2008. Use of fourier transform infrared (FTIR) spectroscopy to study cadmium-induced changes in padina tetrastromatica (hauck). Anal. Chem. Insights 3, 117739010800300001.

Dranguet, P., et al., 2017. Mercury Bioavailability, Transformations, and Effects on Freshwater Biofilms, vol. 36, pp. 3194–3205.

Fleming, E.J., et al., 2006. Mercury methylation from unexpected sources: molybdate-inhibited freshwater sediments and an iron-reducing bacterium. Appl. Environ. Microbiol. 72, 457–464.

Giordano, M., et al., 2001. Fourier Transform Infrared Spectroscopy as a novel tool to investigate changes in intracellular macromolecular pools in the marine microalga Chaetoceros muellerii (Bacillariophyceae). J. Phycol. 37, 271–279.

Guédron, S., et al., 2020. Diagenetic production, accumulation and sediment-water exchanges of methylmercury in contrasted sediment facies of Lake Titicaca (Bolivia). Sci. Total Environ. 138088.

Guédron, S., et al., 2014. (Methyl) mercury, arsenic, and lead contamination of the world's largest wastewater irrigation system: the mezquital valley (hidalgo state—Mexico). Water, Air, & Soil Pollut. 225, 2045.

Guédron, S., et al., 2017. Mercury contamination level and speciation inventory in Lakes Titicaca & Uru-Uru (Bolivia): current status and future trends. Environ. Pollut. 231, 262–270.

Gupta, V.K., Rastogi, A., 2008a. Biosorption of lead(II) from aqueous solutions by non-living algal biomass Oedogonium sp. and Nostoc sp.—a comparative study. Colloids Surf. B Biointerfaces 64, 170–178.

Gupta, V.K., Rastogi, A., 2008b. Equilibrium and kinetic modelling of cadmium(II) biosorption by nonliving algal biomass Oedogonium sp. from aqueous phase. J. Hazard Mater. 153, 759–766.

Gupta, V.K., Rastogi, A., 2009. Biosorption of hexavalent chromium by raw and acid-treated green alga Oedogonium hatei from aqueous solutions. J. Hazard Mater. 163, 396–402.

Gupta, V.K., et al., 2010. Biosorption of nickel onto treated alga (Oedogonium hatei): application of isotherm and kinetic models. J. Colloid Interface Sci. 342, 533–539.

Krauss, F., Schmidt, A., 1987. Sulphur sources for growth of Chlorella fusca and their influence on key enzymes of sulphur metabolism. Microbiology 133, 1209–1219.

Lanza, W.G., et al., 2017. Association of a specific algal group with methylmercury accumulation in periphyton of a tropical high-altitude andean lake. Arch. Environ. Contam. Toxicol. 72, 1–10.

Lázaro, W.L., et al., 2013. Cyanobacteria enhance methylmercury production: a hypothesis tested in the periphyton of two lakes in the Pantanal floodplain, Brazil. Sci. Total Environ. 456–457, 231–238.

Leclerc, M., et al., 2015. Relationship between extracellular low-molecular-weight thiols and mercury species in natural lake periphytic biofilms. Environ. Sci. Technol. 49, 7709–7716.

Liu, J.J., et al., 2016. Variations of effective volume and removal rate under different water levels of constructed wetland. Ecol. Eng. 95, 652–664.

Luoma, S.N., Rainbow, P.S., 2005. Why is metal bioaccumulation so variable? Biodynamics as a unifying concept. Environ. Sci. Technol. 39, 1921–1931.

Mason, R.P., et al., 1996. Uptake, toxicity, and trophic transfer of mercury in a coastal diatom. Environ. Sci. Technol. 30, 1835–1845.

Mays, P.A., Edwards, G.S., 2001. Comparison of heavy metal accumulation in a natural wetland and constructed wetlands receiving acid mine drainage. Ecol. Eng. 16, 487–500.

Miles, C.J., et al., 2001. Partitioning of monomethylmercury between freshwater algae and water. Environ. Sci. Technol. 35, 4277–4282.

Mitsch, W.J., Wise, K.M., 1998. Water quality, fate of metals, and predictive model validation of a constructed wetland treating acid mine drainage. Water Res. 32, 1888–1900.

Molina, C.I., et al., 2010. Transfer of mercury and methylmercury along macroinvertebrate food chains in a floodplain lake of the Beni River, Bolivian Amazonia. Sci. Total Environ. 408, 3382–3391.

Moye, H.A., et al., 2002. Kinetics and uptake mechanisms for monomethylmercury between freshwater algae and water. Environ. Sci. Technol. 36, 3550–3555.

Moye, H.A., et al., 2003. Erratum: kinetics and uptake mechanisms for monomethylmercury between freshwater algae and water. Environ. Sci. Technol. 37, 1056-1056.

Pickhardt, P.C., Fisher, N.S., 2007. Accumulation of inorganic and methylmercury by freshwater phytoplankton in two contrasting water bodies. Environ. Sci. Technol. 41, 125–131.

Sarret, G., et al., 2019. Extreme arsenic bioaccumulation factor variability in lake Titicaca, Bolivia. Sci. Rep. 9, 10626.

Sheath, R.G., Wehr, J.D., 2015. Chapter 1 - Introduction to the Freshwater Algae. Freshwater Algae of North America, second ed. Academic Press, Boston, pp. 1–11.

Skrobonja, A., et al., 2019. Uptake kinetics of methylmercury in a freshwater alga exposed to methylmercury complexes with environmentally relevant thiols. Environ. Sci. Technol. 53, 13757–13766.

Team, R.C., 2013. R: A Language and Environment for Statistical Computing. R Foundation for Statistical Computing, Vienna, Austria.

Val, J., et al., 2016. Influence of global change-related impacts on the mercury toxicity of freshwater algal communities. Sci. Total Environ. 540, 53–62.

Wang, Y., et al., 2018. Adsorption of methylmercury onto geobacter bemidijensis bem. Environ. Sci. Technol. 52, 11564–11572.

Wetzel, R.G., Likens, G.E., 2000. Composition and biomass of phytoplankton. In: Wetzel, R.G., Likens, G.E. (Eds.), Limnological Analyses. Springer New York, New York, NY, pp. 147–174.